This is a peer-reviewed, accepted author manuscript of the following article: Venuturumilli, S., Berg, F., Zhang, M., & Yuan, W. (2020). Investigation of HTS cable impact on turboelectric aircraft performance. *IET Electrical Systems in Transportation*, *10*(1), 62-67. https://doi.org/10.1049/iet-est.2018.5095

Investigation of HTS cable impact on Turbo-Electric Aircraft Performance

Sriharsha Venuturumilli [1*], Frederick Berg [2], Min Zhang [1] and Weijia Yuan [1*]

[1] Electronics and Electrical Engineering Department, University of Strathclyde, Glasgow, U.K.
[2] Airbus E-Aircraft Systems, Munich, Germany
[*]sriharsha.venuturumilli@strath.ac.uk & weijia.yuan@strath.ac.uk

Abstract: With significant interest in the use of high temperature superconducting (HTS) components in electric aircraft, there is a need for novel modelling techniques that allow architecture-level studies of the electrical systems including HTS components. In this paper, a simple electric network architecture, as proposed in the literature has been considered, which includes Generators, dynamic Propulsion load and Cables. This Electric Network has been modelled considering conventional technology and using HTS cables by replacing the conventional copper cables, to evaluate the variations in the network performance. The network performance has been studied for the dynamically varying propulsion load, which is nearly equivalent to the aircraft load over the entire flight duration. Following this, Electric Faults have been applied at various locations and the impact of HTS cables on the network fault levels have been evaluated. The fault current levels are compared using both conventional and HTS cables, due to the fault current limiting properties of the HTS cables, they are observed to offer lowered fault current values.

1. Introduction

Global air traffic passenger demand has been steadily increasing over the last decade, at a yearly average rate of 5.4% [1]. With steady increase in air traffic and increased atmospheric pollution, stringent emissions targets were imposed by the aviation authorities for the next generation aircraft technologies, resulting in a demand for alternate aircraft propulsion technologies.

'More electric' aircraft technologies were already a reality, with hydraulic and pneumatic systems being partly replaced with electrical solutions [2]. Significant research is currently being focused on electric aircraft propulsion as a possible avenue for improving efficiency and emissions.

NASA has been a pioneer in pushing the turbo-electric distributed propulsion (TeDP) technology, in collaboration with major aerospace companies [3-7]. They have published several aircraft studies, which includes: use of boundary layer ingestion (BLI) to improve propulsion efficiency and using large quantities of batteries as a source of propulsive power. However, although these studies show possible ways of using electric propulsion, there are still certain technological challenges to be considered. Electrical components must be redesigned for aeronautical application [8,9], and there is a need for lightweight distribution systems to transmit power within the aircraft.

Simple force balance calculations can show that even small commercial passenger aircraft will require 10s of MVA of propulsion power [9,10]. For transferring such a huge power along the body of an aircraft, conventional copper cables were no longer feasible due to weight/efficiency restrictions. With light weight, negligible losses and large power densities, HTS (High Temperature Superconducting) cables have been proposed for this application. HTS cables have already been installed in various power grids world-wide, and also in ships for specific applications [11-13].

Based on accuracy, efficiency and complexity of the application, several modelling platforms and ideas have been proposed for applied superconductivity. Saying this, in regards to cables, there is a huge need for fast responding models, but with considerable accuracy range. Several attempts have been made in the literature, but they are limited only to the electrical domain modelling of HTS cables [14]. In this paper, a new electrical and thermal coupled superconducting cable model, in regards to the triaxial cable design is proposed.

With very few manufacturers and stigma behind the application of HTS cables, there is a need for more research to understand their performance under various circumstances, particularly for the dynamic aircraft propulsion energy demand. The use of HTS devices on board the aircraft was investigated in the literature, but was limited only to feasibility studies from the scope of mass, efficiency and cryogenic design [15, 16]. While, for the first time this paper simulates the performance of a conceptual turbo-electric aircraft power system with HTS cables. Similarly, a thermo-electric cable model for the HTS cable is presented for the first time in this paper, using the analytical approach. The dynamic resistance characteristics of the HTS cable model are studied, which proves the cable model to be robust and reliable. This paper also investigates the quench performance of HTS cables under the fault current scenarios inside the aircraft power system. The fault current levels of the electric aircraft's network are invested using both HTS and copper cables, emphasising the importance of the HTS cables in the overall network performance

2. Turbo-Electric Aircraft Architecture

Use of electric machines for propulsion purpose in place of high performance engines, would redefine the aircraft power system architecture. Based on the feasibility studies carried out by NASA in collaboration with Rolls-Royce, a few top level architecture designs have been put forward [17,18]. They are listed as DC, AC-DC and AC, based on the transmission system voltage type with each having their own pros and cons. The AC candidate

This is a peer-reviewed, accepted author manuscript of the following article: Venuturumilli, S., Berg, F., Zhang, M., & Yuan, W. (2020). Investigation of HTS cable impact on turboelectric aircraft performance. *IET Electrical Systems in Transportation*, *10*(1), 62-67. https://doi.org/10.1049/iet-est.2018.5095

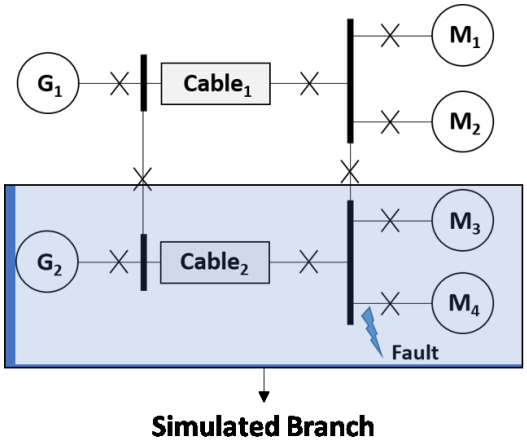

Fig. 1. Single line diagram of the proposed architecture of Turbo-Electric Aircraft, where 'G' stands for generator, 'M' for motor and 'X' for C.B.'s.

architecture stands out to be unique, with high efficiency and drastically reduced mass due to the removal of power electronics, compared to the AC-DC and DC candidate architectures. Although there are problems associated with an architecture of this type, we adopt a similar concept in this initial study to avoid undue complexity.

For now, we also use conventional machines in our architecture to avoid the complexity of modelling the superconducting machines. Being the early stages of modelling the network performance of the electric aircraft propulsion system, no protection or fault clearance strategies have been included in this model as shown in Fig. 1. Thus, the circuit breakers (C.B.) were assumed to be not operating under the fault scenario, letting the fault to be present for the entire 5 cycles duration and also the loss from C.B.'s is assumed to not effecting the temperature of HTS cables. Thus with bus ties being considered as open, the simulated branch was as shown in Fig. 1.

The idea behind this selected architecture for the aircraft was based on a consideration that there will be two different power systems inside the aircraft, one being the propulsion power system operating at medium voltage (600 V- 69 kV) [17], while the normal utility power system is separate and being operated at low voltage (< 600 V). This makes sense in terms of aircraft manufacturing, as the passengers will be exposed to the maximum of normal

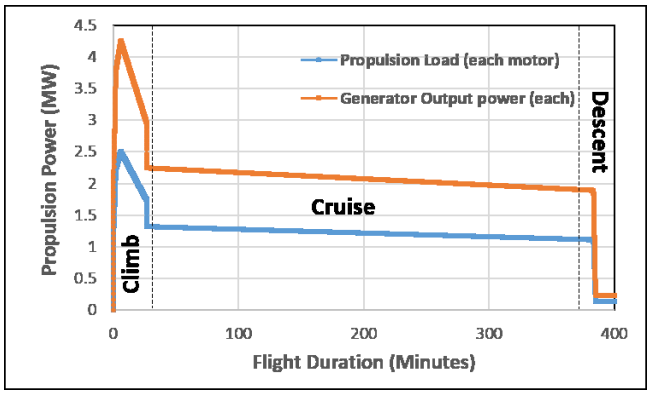

Fig. 2. Dynamic Propulsion load of a typical conventional Aircraft.

operating low voltage and also removes the need for extra converters/transformer inside the aircraft, which requires extra room and adds significant weight.

The proposed architecture has been modelled in Matlab/Simulink with two generators feeding in the power to the four Propulsion motors with the combined maximum power demand of 10 MW. The generator was assumed to be an unsaturated salient pole synchronous machine model for this study. The unique characteristic of the aircraft power demand is its dynamic nature, which varies from zero to its maximum power within a very short time. To simulate its characteristics, a similar propulsion demand curve has been imposed on the load uniformly as shown in Fig. 2.

3. HTS Cable Model

Superconducting materials were well known for their highly non-linear and exponential properties, which make it very difficult to model them for engineering applications. A wide variety of software's have been used in literature to model the superconducting properties, which can be broadly categorized into software's solving for field models and circuit models. With each having their pros and cons, field models are still not capable of solving the system level models. For architectural level modelling, signal-based methods are suitable. The models presented in this paper have been implemented in Matlab/Simscape, using the Simulink environment.

Several attempts have been made in literature to model superconducting power appliances, particularly with regard to SFCL and SMES [19,20]. Only a few papers have worked on modelling the superconducting cables, even then they were limited only towards their integration into the power grid applications [21]. Since turbo-electric aircraft propulsion systems were a microgrid, it must be modelled and optimized very carefully, as the failure of the smallest part can lead to a catastrophic failure of the entire grid. In this model, Simscape alone has been utilized to model its properties, which makes it very easy to interconnect it with all other models based on Simscape signals.

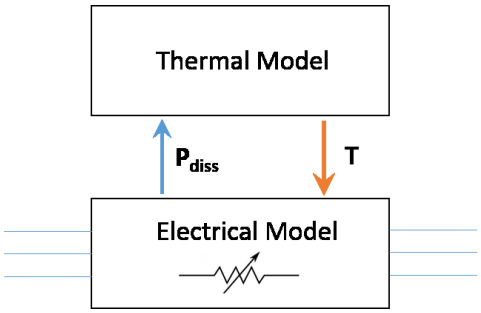

Fig. 3. Layout of the 3 Phase, Triaxial HTS cable in Simscape.

A triaxial cable design has been chosen for this model, cooled down by LN_2 as shown in Fig. 3. Similarly, the parameters employed for modelling the HTS cable are as listed in the Table I. For simplification, the HTS tape is considered to have only the HTS layer and Copper layer, neglecting the other layers in both electrical and thermal

This is a peer-reviewed, accepted author manuscript of the following article: Venuturumilli, S., Berg, F., Zhang, M., & Yuan, W. (2020). Investigation of HTS cable impact on turboelectric aircraft performance. *IET Electrical Systems in Transportation*, *10*(1), 62-67. https://doi.org/10.1049/iet-est.2018.5095

Table 1 Operating parameters of the HTS cable.

Cable Parameters	Value
Rated Voltage	4160 V (rms)
I_C of each phase (@70 K)	2000 A (peak)
Total Length	100 m
Cooling Medium	LN_2 (70 K)

models. As copper and HTS layers being the sole electrically conducting materials within the HTS tape, this assumption was valid electrically. While, neglecting the other layers could possibly impact the thermal characteristics, which was not considered in the present study. The highly nonlinear property of HTS material has been modelled using the E-J power law, according to equation (1)[22].

$$\rho_{HTS} = \frac{E_C}{J_C(T)}\left(\frac{J}{J_C(T)}\right)^{n-1} \quad T < T_C, J < J_C \ (1)$$

where, ρ_{HTS} is the "resistivity of HTS material (Ω.m)", E_c being the "critical electric field (V/m)", T_c being "critical temperature (K)", J_c being the "critical current density (A/m^2)" and n is made equal to 21. The critical current density, J_c of the HTS material does vary w.r.t the operating temperature, T according to equation (2).

$$J_C(T) = J_{C0}\left(\frac{T_C - T}{T_C - T_0}\right)^{1.3} \quad (2)$$

Similarly, the resistivity of the copper also changes with temperature and is modelled according to equation (3).

$$\rho_{Cu} = (0.0084T - 0.4603) \times 10^{-8}, T > T_C \ (3)$$

where, ρ_{Cu} is the "resistivity of copper stabilizer (Ω.m)" and T_c being the critical temperature of the HTS tape. ρ_{Cu} plays the key part during the fault/quench operation. In this paper, the thickness of the copper stabilizer is assumed to be of 50 µm.

The lumped electrical model of the cable is built using the Π configuration as shown in the Fig. 4 and the inductance and capacitance values used in the model are as

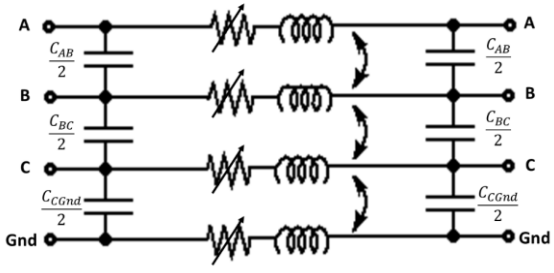

Fig. 4. Lumped electrical network model of the HTS cable built using the Π configuration.

Table 2 Electrical parameters of the HTS cable.

Self-Inductance (µH/km)		Mutual-Inductance (µH/km)		Capacitance (nF/km)	
L_A	152.69	M_{AB}	58.19	C_{AB}	668.83
L_B	93.87	M_{BC}	45.02	C_{BC}	864.52
L_C	48.85	M_{CA}	103.22	C_{CGnd}	796.77

shown in Table 2.

To simulate the thermal properties, the heat source is modelled using the current being propagated in both the copper stabilizer and HTS layer, according to equation (4).

$$P_{diss}(t) = i_{Cu}(t)^2 R_{Cu}(t) + i_{HTS}(t)^2 R_{HTS}(t) \ (4)$$

The power dissipated from the three phases was fed as a heat source to the thermal model, while the operating temperature of the LN_2 is set at 70 K, i.e. somewhat subcooled to improve HTS performance. A 2D HTS cable model is built using COMSOL (a field model), to achieve the AC loss results, to be used inside the analytical model as shown in Fig. 5. Thus using this field model, AC losses for

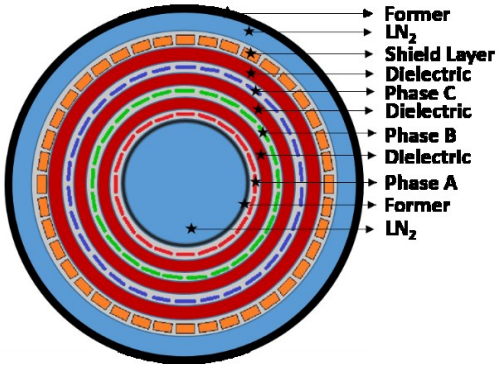

Fig. 5. 2D AC triaxial HTS cable cross-sectional layout used for developing the analytical HTS cable model.

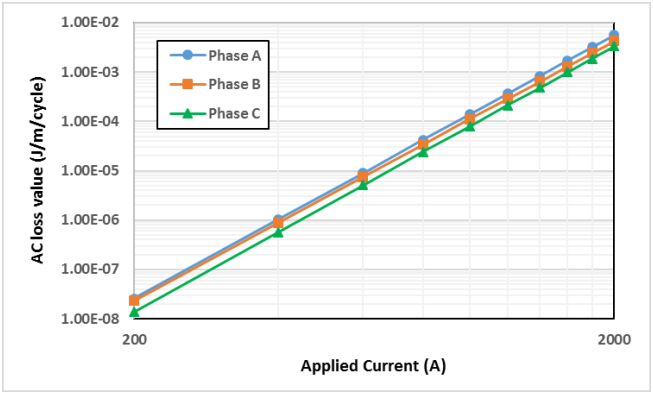

Fig. 6. AC loss values of the HTS cable for varying applied current values.

This is a peer-reviewed, accepted author manuscript of the following article: Venuturumilli, S., Berg, F., Zhang, M., & Yuan, W. (2020). Investigation of HTS cable impact on turboelectric aircraft performance. *IET Electrical Systems in Transportation*, *10*(1), 62-67. https://doi.org/10.1049/iet-est.2018.5095

the particular geometry with varied applied currents have been modelled and are given as a function of applied current as seen in Fig. 6.

The heat model has been modelled for the first time using the Simscape thermal components, which will significantly improve the accuracy of the results. The parameters of the heat model were made as variables and the values of thermal conductivity and specific heat were defined as a function of temperature [23]. Considering a uniform heat flow in the radial direction through several layers of the HTS cable, the thermal conduction process along the solid layers is modelled by using the equation (5)

$$q(\Delta T) = A \times \lambda \times \frac{\Delta T}{\Delta x} \quad (5)$$

where, ΔQ is the "heat transferred (W)", A being the "cross-sectional area of the layer (m^2)", ΔT is the "difference in temperature across the layers (K)", Δx is the "thickness of the layer (m)" and λ is the "thermal conductivity of the layer (W/(m.K))". Similarly, whenever a certain heat is applied, the layer absorbs it to a certain extent before transferring it to the next adjacent layer. This was defined as the thermal mass and was modelled as shown in the equation (6).

$$q(\Delta T) = m \times C_p \times \Delta T \quad (6)$$

where, m is the "mass of the conduction layer (kg)", C_p is the "specific heat (W/(kg.K))". Similarly, the thermal conduction between the LN_2 and the cryostat wall is modelled using a convective heat transfer equation, as shown in equation (7).

$$q(\Delta T) = A \times h \times \Delta T \quad (7)$$

where, h is the "heat transfer coefficient of the LN_2 medium ($W/(m^2.K)$)". It has been found in the literature that the heat transfer co-efficient of LN_2 does vary w.r.t. operating temperature, which makes it very critical for quench modelling [24]. Thus the heat transfer coefficient 'h' of LN_2 has been also modelled as a variable as shown in Fig. 7.

To evaluate the characteristics of the cable, a ramping DC current (1000 A/sec) was applied across every layer with the other layers short-circuited. The resistance characteristics of the HTS cable model with applied current

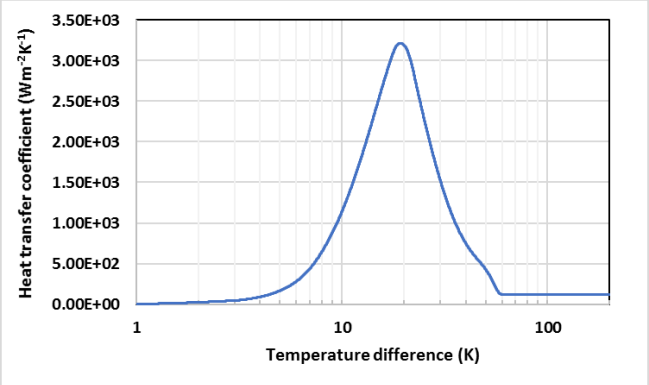

Fig. 7. Variable heat transfer coefficient of the LN_2 [23].

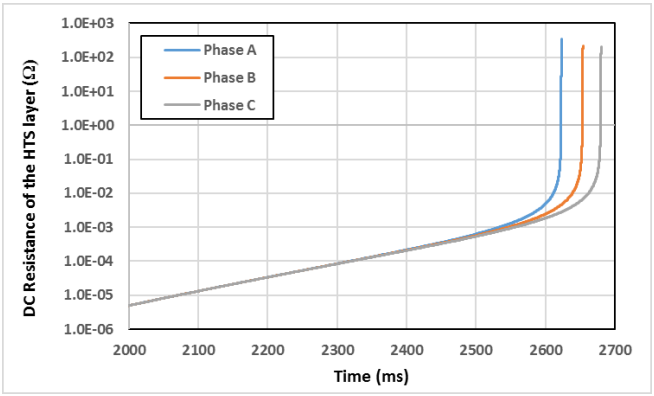

Fig. 8. Variable resistance characteristics of the 3-Phase HTS AC cable.

is as shown in Fig. 8. The minimum resistance offered by the HTS layer for the applied current was observed to be as low as 1E-30 Ω from the HTS cable model. It was observed that these characteristics do change with the ramping rate, resulting in varied operating temperatures thus leading to varied resistance characteristics with applied current.

4. Network Performance

The turbo-electric propulsion network as seen in Fig. 1 with the HTS cables has been modelled under the dynamic loading condition as shown in Fig. 2. The two generators are observed to power the motors without any ripples and the power output of the generators is similar to the load profile, as shown in Fig. 2. The generators, each were rated for 10 MVA peak capacity, considering redundant operation. Thus, under normal conditions, each generator was loaded to a maximum power of 5 MVA, with the HTS cable loaded to a peak current of 1000 A. A R-L load was used to simulate dynamic propulsion load of the motors, with a power factor of 0.9. This assumption undermines the variable frequency response of the power system, as the frequency of the power system was supposed to vary in accordance with the power demand, with the motors and generators being synchronised. But, the current study was limited to the fault current response and this assumption will not have any impact on the achieved results.

In order to understand the dynamic stability of the network under different fault conditions, i.e. both symmetrical (LLL-G and LLL) and unsymmetrical (L-G, LL and LL-G) faults have been simulated.

4.1. Under Single phase to Ground (L-G) fault

A single phase to ground fault has been introduced at the terminations of motor 4, under the climb scenario as seen in Fig. 1 and Fig. 2. A short-circuit fault with a resistance of 1 mΩ was simulated for a duration of 5 cycles, to understand the performance of generators and HTS cable characteristics in the network during the fault period. The generator was also observed to get affected in its

This is a peer-reviewed, accepted author manuscript of the following article: Venuturumilli, S., Berg, F., Zhang, M., & Yuan, W. (2020). Investigation of HTS cable impact on turboelectric aircraft performance. *IET Electrical Systems in Transportation*, *10*(1), 62-67. https://doi.org/10.1049/iet-est.2018.5095

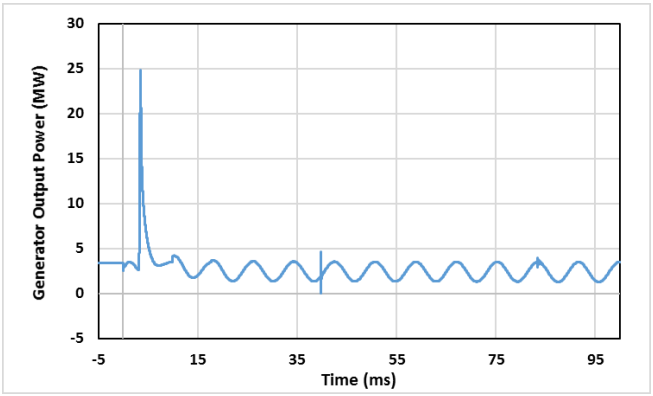

Fig. 9. Output power of generator 2, during the fault condition.

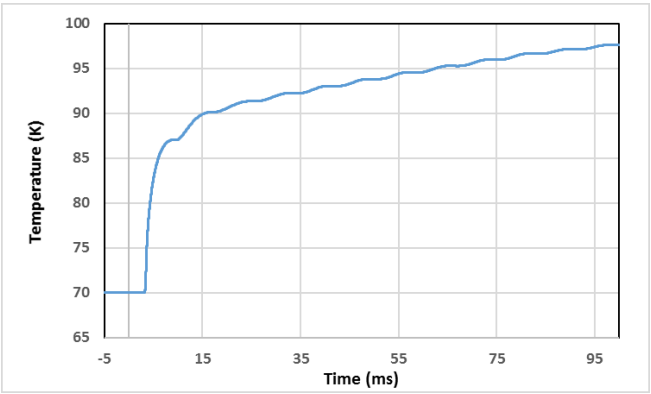

Fig. 11. Temperature profile of the HTS cable during the fault condition.

performance during the fault current and a pulsated power output, resulting from the sudden increase in the resistance of the HTS cable. During the residual fault period, a significant amount of ripple was observed in the generator output as shown in Fig. 9.

Similarly, the voltage and current profiles of the network, during the fault were as seen in Fig. 10. The maximum fault current magnitude generated was observed as 3.5 kA. The fault current was observed to be limited, due to the fault current limiting characteristics of the HTS cable.

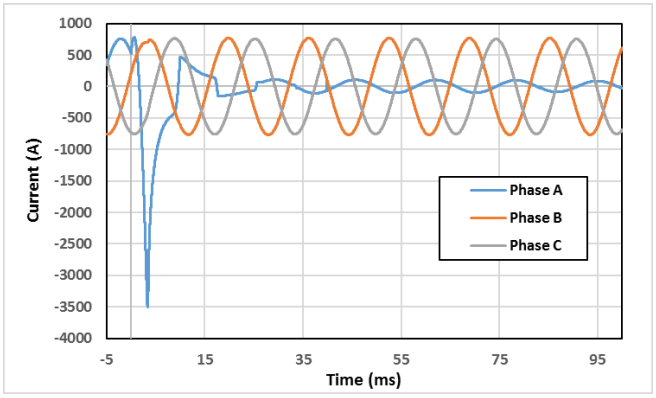

(a)

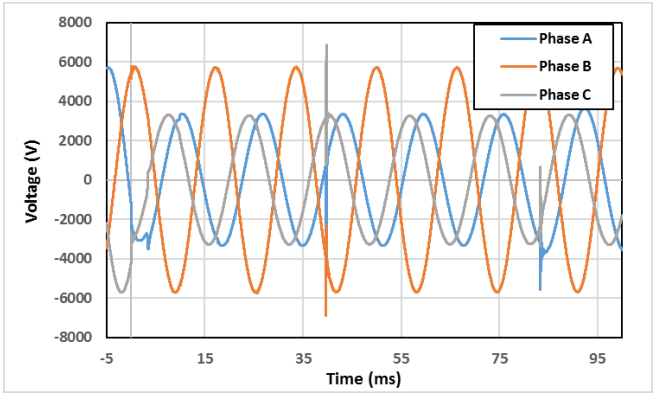

(b)

Fig. 10. Current (a) and Voltage (b) characteristics of the electric network, under fault duration using HTS cable.

From Fig. 11, it was observed that the temperature of the phase A superconducting layer increased, leading to a reduced critical current rating of the HTS as seen in equation (2), thus increasing the HTS resistance exponentially following the equation (1).

Beyond 93 K, finally HTS loses its superconductivity property, thus forcing the entire current into the copper stabilizer. This sudden change in resistance could cause a ripple as observed in the voltage curve of the Fig. 10, between 30-35 ms duration. In this paper, the fault current is simulated only for 5 cycles, but under continued operation, the cable is observed to remain in a quench state with the temperatures reaching up to as high as 600 K, which can lead to the permanent damage of cable. Hence, a circuit breaker was required in series to the cable, designed to operate at the immediate zero crossing, after the fault inception.

4.2. Under all other faults

Similar analysis has been done on the network model for all the other faults. For the comparison purpose, the network model has been simulated with the conventional copper cable model as well. Considering the large ampacity

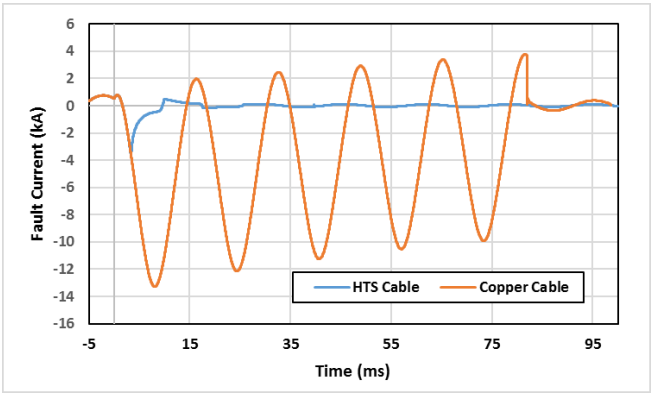

Fig. 12. Comparison of fault currents experienced by phase A of electric network using both HTS and Copper cables for an L-G fault.

This is a peer-reviewed, accepted author manuscript of the following article: Venuturumilli, S., Berg, F., Zhang, M., & Yuan, W. (2020). Investigation of HTS cable impact on turboelectric aircraft performance. *IET Electrical Systems in Transportation*, *10*(1), 62-67. https://doi.org/10.1049/iet-est.2018.5095

requirements, three independent cables were assumed for three given phases. The parameters of the copper cable were set as 20 mΩ/km, 500 μH/km and 300 nF/km. A phase – ground short circuit fault was introduced at the propulsion load terminals, leading to a sharp increase in the fault current magnitude within the phase A. Fig. 12 shows the comparison between the fault currents experienced by the phase A of the electric aircraft network, employing both HTS and copper cables. The fault current magnitude of the HTS cable was limited to only 3.5 kA due to the quench, while the fault current magnitude employing the copper cable has reached as high as 13.3 kA with no means to control it. Similarly, various other kinds of faults have been introduced and the corresponding fault current values have been summarized in the Table 3, quantifying the maximum fault current magnitude using both copper and HTS cables.

Table 3 Fault current rating of electric aircraft network for typical power system faults.

Fault type	Maximum fault current magnitude (kA)	
	Copper cable	HTS cable
L-G	13.3	3.5
LL	10.2	3.56
LL-G	12.2	3.6
LLL	11.4	3.5
LLL-G	10.3	3.6

5. Conclusions

A simple turbo-electric aircraft propulsion network has been modelled in this paper, giving a good insightful knowledge of the network performance under the normal and fault current scenarios. It has been observed that, irrespective of the time of fault occurrence (i.e. climb, cruise and descent states), there was not much change in the fault magnitude and machine performance.

The developed HTS cable model was observed to work very efficiently, offering negligible resistance during the normal condition and increasing exponentially with fault current without any convergence problems. Using this novel model, the entire network has been modelled for all faults, giving detailed information of the reliability of HTS cable performance under various electrical faults and the figures were shown in particular to single phase to ground (L-G) fault. The HTS cables were observed to quench the fault current magnitude by $1/5^{th}$ of the copper cable results, thus reducing the rating of the switchgear required inside the electric network. It was observed that the maximum fault current rating and heat dissipated inside the HTS cable can be controlled by the design and also with the rating of the HTS cable.

Certain assumptions have been made in this paper, which includes: LN_2 input and output temperature to be constant and unlimited cooling capacity, Ic value to be uniform along the entire length of cable and the generators to power the propulsion motors separately, rather than in a synchronous manner. As a part of future work, the cable needs to be modelled as a distributed model and needs to be investigated for quench propagation, to optimize the Circuit Breaker operating conditions. Similarly, the performance of the generators operating in a synchronous manner under the influence of fault scenarios, needs to be investigated, highlighting the current sharing phenomena among the cables as well. The models developed can be reconfigured into different architectures, thus leaving a wide variety of research scope to the present study. The addition of other superconducting components, as well as converters, will allow more complex propulsion systems to be modelled.

6. Acknowledgments

This work has been part funded by Airbus Group.

7. References

[1] IATA, 'Annual Growth in Global Air Traffic Passenger Demand from 2005 to 2017,' Statista - The Statistics Portal, Statista, www.statista.com/statistics/193533/growth-of-global-air-traffic-passenger-demand/, Accessed on: June. 07, 2019

[2] Sinnet, M.: '787 No-Bleed Systems: Saving Fuel and Enhancing Operational Efficiencies,' Aero magazine, http://www.boeing.com/commercial/aeromagazine/articles/qtr_4_07/AERO_Q407_article2.pdf, Accessed on: June. 07, 2019.

[3] Bradley, M.K., and Droney, C.K.: 'Subsonic Ultra Green Aircraft Research: Phase I Final Report,' NASA CR-2011-216847, 2011.

[4] Greitzer, E. M., Bonnefoy, P.A., De la Rosa Blanco, E., et al.: 'N+3 Aircraft Concept Designs and Trade Studies,' NASA CR-216794/VOL1, 2010.

[5] Bruner, S., Baber, S., Harris, C., et al.: 'NASA N+3 Subsonic Fixed Wing Silent Efficient Low-Emissions Commercial Transport (SELECT) Vehicle Study,' NASA CR-2010-216798, 2010.

[6] D'Angelo, M. M., Gallman, J., Johnson, V., et al.: 'N+3 Small Commercial Efficient and Quiet Transportation for Year 2030- 2035,' NASA CR-2010-216691, 2010.

[7] Felder, J., Kim, H. and Brown, G.: 'Turboelectric Distributed Propulsion Engine Cycle Analysis for Hybrid-wing-body Aircraft,' AIAA 2009-1132, 2009.

[8] Siemens, 'Electric propulsion components with high power densities for aviation,' Siemens - Transformative Vertical Flight Workshop, https://nari.arc.nasa.gov/sites/default/files/attachments/Korbinian-TVFW-Aug2015.pdf, accessed on: June 07 2019.

[9] E-Fan X project, 'Airbus, Rolls-Royce, and Siemens team up for electric future,' https://www.siemens.com/press/en/pressrelease/?press=/en/pressrelease/2017/corporate/pr2017110098coen.htm. accessed on: June 07 2019.

[10] Borst, C., Sjer, F. A., Mulder, M., et al.: 'Ecological approach to support pilot terrain awareness after total engine failure,' Journal of Aircraft, 2012, 45, (1), pp 159–171.

[11] Miller, J., Santosusso, D., Uva, M., et al.: 'Naval superconducting integrated power system,' Proc. Intell. Ships Symp., 2013, pp 1-8.

[12] Stemmle, M., Merschel, F., Noe, M., and Hobl, A.: 'Ampacity project—Worldwide first superconducting cable and fault current limiter installation in a German city center,' Proc.22nd Int. Conf. Exhib. Elect. Distrib. 2013, pp 1-4.

[13] Malozemoff, A. P., Yuan, J., and Rey, C. M.: 'High-Temperature Superconducting (HTS) AC Cables for Power Grid Applications', in Ray, C.: 'Superconductors in the Power Grid' (Elsevier, New York, 2015), pp. 133-188.

[14] Yin, L., Ma, X., Li, X., et al.: 'Overcurrent Analysis of YBCO Cable Under Fault Current,' IEEE Transactions on Applied Superconductivity, 26, (7), 2016, pp 1-5.

[15] Berg, F., Palmer, J., Miller, P., and Dodds, G.: 'HTS System and Component Targets for a Distributed Aircraft Propulsion System,' IEEE Transactions on Applied Superconductivity, 27, (4), 2017, pp 1-7.

[16] Berg, F., Palmer, J., Miller, P., et al.: 'HTS Electrical System for a Distributed Propulsion Aircraft,' IEEE Transactions on Applied Superconductivity, 25, (3), 2015, pp 1-5.

[17] Armstrong, M. J., Blackwelder, M., Bollman, A., et al.: 'Architecture, Voltage and Components for a Turboelectric Distributed Propulsion Electric Grid,' NASA CR-2015-218440, 2015.

[18] Jones, C. E., Norman, P. J., Galloway, S. J., et al.: 'Comparison of Candidate Architectures for Future Distributed Propulsion Aircraft,' IEEE Transactions on Applied Superconductivity, 26, (6), 2016, pp 1-9.

[19] Liang, F., Yuan, W., Zhang, M., et al.: 'AC loss modelling and experiment of two types of low-inductance solenoidal coils,' Superconductor Science and Technology, 29 (11), 2016, pp 115006 (1-18).

[20] Li, J., Zhang, M., Yang, Q., et al.: 'SMES/battery hybrid energy storage system for electric buses,' IEEE Transactions on Applied Superconductivity, 26 (4), 2016, 5700305 (1-5).

[21] Del-Rosario-Calaf, G., Lloberas-Valls, J., Sumper, A., et al.: 'Modeling of Second Generation HTS Cables for Grid Fault Analysis Applied to Power System Simulation,' IEEE Transactions on Applied Superconductivity, 23, (3), 2013, pp 5401204-5401204.

[22] Morandi, A.: '2D electromagnetic modelling of superconductors,' Superconductor Science and Technology, 25 (10), 2012, pp 104003 (1-23).

[23] Zhang, M., Matsuda, K., and Coombs, T. A.: 'New application of temperature-dependent modelling of high temperature superconductors: Quench propagation and pulse magnetization,' J. Appl. Phys., 112, (4), 2012, pp 043912 (1-8).

[24] Jin, T., Hong, J., Zheng, H., et al.: 'Measurement of boiling heat transfer coefficient in liquid nitrogen bath by inverse heat conduction method,' J. Zhejiang Univ. Sci. A, 10, (5), 2009, pp 691-696.